Modeling of internal wave generation near a shelf slope by ocean finite element method

Kwi-Joo LEE, Soon-Won JOA* and Ki Chang EOM

Department of Naval Architecture & Ocean Engineering, Chosun University, Gwangju 501-759, Korea

The 3-D modeling of ocean finite element method(OFEM) using k-ε turbulent model and tetrahedron grids has been used to investigate the internal wave generation during the expansion of the deep water from the open sea to the shelf with a simple shape, which can be widely used in the fields of submarine development, ocean environment and meteorology, etc. In this paper, the detailed configuration of internal wave with its length and height and also the distribution of salinity and turbulent kinematic energy, etc. were derived. It is hoped that this OFEM method can be successfully applied to the numerical calculation of internal wave for and the oceanographic problems (tidal flows around underwater hill, plateau, Georges Bank, etc.) and ocean engineering problems(flow past artificial sea reefs) in future.

Key words : OFEM, Numerical calculation, Internal wave, Shelf

Introduction

It is known that Internal wave is generated in the interior of the ocean when the water body consists of layers of different density and it has the huge energy. Thus recently various studies on it are being done for the applicability in the field of submarine development, ocean environment and meteorology, etc.

In this paper representing the basic step of the study on the numerical calculation of internal wave, the 3 – D modeling of ocean finite element method using k – ε turbulent model and tetrahedron grids has been set up to investigate the internal wave generation during the expansion of the deep water from the open sea to the shelf and then the numerical calculation of internal wave is tried to execute with the discussion of calcula – tion results. Using this OFEM, the detailed configura – tion of internal wave with its length and height was successfully derived and also the distribution of salinity and turbulent kinematic energy, etc. were discussed.

Topography of a shelf and the configuration of generated grids

The topography of the shelf for the numerical calculation in this paper is the simple shape of a square pillar of 4,000m × 220m × 10,000m as shown in Fig.1, where the configuration of the section of the shelf is a quadrilateral with an about 80° declination of one side. the period of the tide with 12.4 hours is

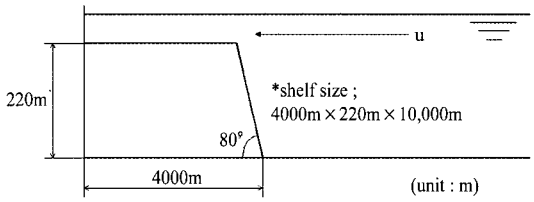

Fig. 1. Configuration of the shelf.

*Corresponding author: joasw@chosun.ac.kr Tel: 82-62-230-7275 Fax: 82-62-227-9942

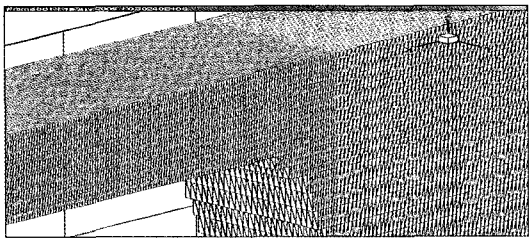

Fig. 2. Configuration of grids generated near the shelf zone.

used as the M2 Tidal forcing.

And the tidal velocity(u) toward the shelf is assu med as 0.6 m/sec.

Grids are generated over the range of x − axis = − 60,000 ~ 40,000 m(space = 200), y − axis = 0 ~ 5,000m(space = 13), z − axis = 0 ~ 2,800 m(space = 10) respectively.

Then near the shelf zone the nest grids are thickened up to 4 m in the horizontal and 1 m in the vertical direction for better performance of numerical calcul ation as shown in Fig. 2.

The basic equations

The basic equations have been cast in modified sigma coordinate system

$$x_1 = x,\ x_2 = y,\ \sigma = a \cdot z,\ t = t \tag{1}$$

The constant a is a scale factor that is relation of horizontal dimension to vertical one. After conversion to sigma coordinates, the basic equations may be written,

$$\frac{\partial u_j}{\partial x_j} + a\frac{\partial w}{\partial \sigma} = 0,$$

$$\frac{\partial u_i}{\partial t} + u_j\frac{\partial u_i}{\partial x_j} + aw\frac{\partial u_i}{\partial \sigma} = -\frac{1}{\rho}\frac{\partial p}{\partial x_i} + f\varepsilon_{ijk}u_i + \frac{\partial}{\partial x_j}\left[(v_H)\frac{\partial u_i}{\partial x_j}\right] + a^2\frac{\partial}{\partial \sigma}\left[(v_e)\frac{\partial u_i}{\partial \sigma}\right],$$

$$\frac{\partial w}{\partial t} + u_j\frac{\partial w}{\partial x_j} + aw\frac{\partial w}{\partial \sigma} = -\frac{a}{\rho}\frac{\partial p}{\partial \sigma} - g + \frac{\partial}{\partial x_j}\left[(v_H)\frac{\partial w}{\partial x_j}\right] + a^2\frac{\partial}{\partial \sigma}\left[(v_e)\frac{\partial w}{\partial \sigma}\right],$$

$$i, j = 1, 2 \tag{2}$$

where, u_i is component of horizontal velocity, w is vertical component of velocity, p pressure, ρ density, v_e vertical eddy viscosity, v_H horizontal eddy viscosity, f parameter of Carioles, $f\varepsilon_{ijk}u_i$ component of asymmetric tensor.

The pressure p can be separated on hydrostatic and non − hydrostatic(dynamic) parts (Mahadevan et al., 1996)

$$p = p_H + p_D, \tag{3}$$

where

$$p_H = \int_0^{\zeta} \rho g dz \tag{4}$$

is hydrostatic part and p_D is dynamic part, ζ is free surface elevation, respectively. The transport equations for salinity and temperature is written as

$$\frac{\partial S}{\partial t} + u_j\frac{\partial S}{\partial x_j} + aw\frac{\partial S}{\partial \sigma} = \frac{\partial}{\partial x_j}\left[(v_H/Pr)\frac{\partial S}{\partial x_j}\right] + a^2\frac{\partial}{\partial \sigma}\left[(v_e/Pr)\frac{\partial S}{\partial \sigma}\right], \tag{5}$$

$$\frac{\partial T}{\partial t} + u_j\frac{\partial T}{\partial x_j} + aw\frac{\partial T}{\partial \sigma} = \frac{\partial}{\partial x_j}\left[(v_H/Pr)\frac{\partial T}{\partial x_j}\right] + a^2\frac{\partial}{\partial \sigma}\left[(v_e/Pr)\frac{\partial T}{\partial \sigma}\right], \tag{6}$$

where is P_r Prandtl number. The vertical eddy viscosity v_e can be expressed as a sum of molecular viscosity v and turbulent viscosity v_t. So, according to Kolmogorov' hypothesis we have

$$v_e = v + v_t = v + c_n\frac{K^2}{\varepsilon} \tag{7}$$

where, k is turbulent kinetic energy, and ε its dissipation rate, $C_n = 0.09$. The dissipation rate can be represented in the form $\varepsilon = k/\lambda$, where l is turbulent scale. It is useful for the definition of initial value of dissipation rate. The turbulent parameters are the scalars and can be found from transport equations

$$\frac{\partial K}{\partial t} + u_j\frac{\partial K}{\partial x_j} + aw\frac{\partial K}{\partial \sigma} =$$

$$\frac{\partial}{\partial x_i}\nu_H\frac{\partial K}{\partial x_j}+a^2\frac{\partial}{\partial\sigma}\left[(\nu+\nu_t/Pr_k)\frac{\partial K}{\partial\sigma}\right]+p-\varepsilon, \quad (8)$$

$$\frac{\partial\varepsilon}{\partial t}+u_j\frac{\partial\varepsilon}{\partial x_j}+aw\frac{\partial\varepsilon}{\partial\sigma}= \frac{\partial}{\partial x_i}\nu_H\frac{\partial\varepsilon}{\partial x_j}+a^2\frac{\partial}{\partial\sigma}\left[(\nu+\nu_t/Pr_\varepsilon)\frac{\partial\varepsilon}{\partial\sigma}\right]+1.44\cdot p\cdot\frac{\varepsilon}{k}-1.92\cdot\frac{\varepsilon^2}{k}, \quad (9)$$

where $Pr_k=1.0$, $Pr_\varepsilon=1.3$. This closure is known as "$k-\varepsilon$" model of turbulence [Mathieu and Scott, 2000]. The term P is production of turbulence due to stresses.

The horizontal eddy viscosity is defined according to subgrid scale model of Smagorinsky

$$\nu_t=(C_S\Delta)^2\left|2\left(\frac{\partial u_i}{\partial x_j}+\frac{\partial u_j}{\partial x_i}\right)\left(\frac{\partial u_i}{\partial x_j}+\frac{\partial u_j}{\partial x_i}\right)\right|^{\frac{1}{2}} \quad (10)$$

where $C_s=0.17$, Δ is filter width.

Numerical approximation

Splitting scheme

The difficult of the pressure calculation can be overcome by applying of splitting schemes. Let us introduce the following symbols

$$Adv=uj\frac{\partial}{\partial x_j},\ Dif=\frac{\partial}{\partial x_j}\nu_e\frac{\partial}{\partial x_j},\ Grad=\frac{\partial}{\partial x_j}$$

According to Hirt' splitting scheme the intermediate values of velocity find from equations (Fletcher, 1991)

$$\frac{\tilde{u}_i-u_i^n}{\Delta t}+Aduu_i^n=-\frac{1}{\rho}Grad\,p^n+Dif\,u^n \quad (11)$$

where Δt is time step. The resulting values of velocity are corrected following procedure.

$$u_i^{n+1}=\tilde{u}_i-\Delta t/\rho\ Grad\,(\delta p) \quad (12)$$

where p is pressure correction and solution of Poisson equation

$$\frac{\Delta t}{\rho}\frac{\partial^2(\delta p)}{\partial x_j^2}=\frac{\partial\tilde{u}_i}{\partial x_j} \quad (11)$$

Finite element approximation

We define every unknown variable as the following scalar function.

$$\varphi=[u_i,p,k,\varepsilon]^T:\ \Omega\times[0,T]\to R^n$$

Then, problem (1) – (9) can be rewritten in generalization form

$$\frac{\partial\varphi}{\partial t}+\sum_{i=1}^{n}v_iD_i\varphi-\sum D_i\nu_eD_i\varphi=f$$

in $Q=\Omega\times[0,T]$, $n=3$ (14)

$\varphi=\phi$ in $\Gamma\times[0,T]$ (15)

$\varphi(x,0)=\varphi_0(x)$ in Ω (16)

where

$$D_i=\partial/\partial x_i,\ \nu_e=\nu+C_n\ k^2/(\varepsilon+\varepsilon_0),$$

ϕ is the boundary condition, $\varphi_0(x)$ is the initial condition. The Galerkin' s finite element method can be applied to the equation (14). Approximation of the second order of accuracy can be obtained at the tetrahedron element. This element allows a simple construction of a grid in the complex domain. In the present study we use the following basic functions (Norrie and De Vries, 1978).

$$\Phi_i^e=\frac{1}{6Ve}(a_i^e+a_i^ex+c_i^ey+d_i^ez) \quad (17)$$

where

$$6V_e=\begin{bmatrix}1&x_1&y_1&z_1\\1&x_2&y_2&z_2\\1&x_3&y_3&z_3\\1&x_4&y_4&z_4\end{bmatrix} \quad (18)$$

and coefficients a_i, b_i, c_i, d_i are solution of the system.

$$\begin{bmatrix}1&x_i&y_i&z_i\\1&x_j&y_j&z_j\\1&x_k&y_k&z_k\\1&x_l&y_l&z_l\end{bmatrix}\cdot\begin{bmatrix}a_i^e\\b_i^e\\c_i^e\\d_i^e\end{bmatrix}=\begin{bmatrix}1\\1\\1\\1\end{bmatrix} \quad (19)$$

According to the Galerkin' s method the projection basis and approximation basis belong to one class of function. As a result, we obtain the matrix equation.

$$M\frac{1}{6Ve}+Adv\cdot\varphi+Dif\cdot\varphi=F) \quad (20)$$

with coefficients

$$\varphi=\sum_{m=1}^{M}\varphi_m(t)\,\Omega_m(x,\,y,\,z)$$

$$M=\sum_{m=1}^{M}\int_{\Omega}\varphi_m\varphi_l\,d\,\Omega)$$

$$adv=\sum_{m=1}^{M}\int_{\Omega}\left(v_1^m\frac{\partial\Phi_m}{\partial x_1}+v_2^m\frac{\partial\Phi_m}{\partial x_2}+v_3^m\frac{\partial\Phi_m}{\partial x_3}\right)\Phi_l\,d\Omega$$

$$Dif=\sum_{m=1}^{M}\int_{\Omega}\nu_t\left(\frac{\partial\Phi_m}{\partial x_1}\frac{\partial\Phi_l}{\partial x_1}+\frac{\partial\Phi_m}{\partial x_2}\frac{\partial\Phi_l}{\partial x_2}+\frac{\partial\Phi_m}{\partial x_3}\frac{\partial\Phi_l}{\partial x_3}\right)d\Omega$$

$$F=M$$

$$1\le m,\ l\le M \qquad (21)$$

The classical Galerkin' method does not guarantee the obtaining of solution free from numerical oscillation. The Petrov – Galerkin' procedure lets to improve this situation (Schachverdy,1993).

Initial and boundary conditions

Initial condition

We shall let that at initial time the flow was a rest. The components of the velocities and turbulent characteristics are equal zero

$$u_i(x_i,\,0)=0.0,\ k(x_i,\,0)=0,\ \varepsilon(x_i,\,0)=0 \qquad (26)$$

The dynamical part of pressure can be set a constant

$$P_D=P_{D0} \qquad (27)$$

The hydrostatic part of pressure can be found according to formula

$$P_H=\rho g(\zeta_0-z) \qquad (28)$$

If we put that

$$\zeta_0=const \qquad (29)$$

Boundary condition

On solid walls, we set

$$u_i(x_i,\,t)=0 \qquad (30)$$

and

$$k_w(x_w,\,t)=\tau_w/(\rho c_n^{1/2}),\ \varepsilon_w(x_i,\,t)=c_n^{3/4}k^{3/2}/l \qquad (31)$$

$$\frac{\partial S}{\partial n}\frac{\partial T}{\partial n}=0 \qquad (32)$$

On free surface, the "rigged lid" boundary condition is imposed

$$u_3=0,\ p=p_a \qquad (33)$$

And also kinemaric boundary conditions are as follows.

$$w=0,\ \sigma=0,\ w=u\frac{\delta H}{\delta x}-v\frac{\delta H}{\delta y},\ \sigma=H$$

On outflow and inflow boundaries one of the following types of boundary conditions are imposed.

(i) Cyclical boundary condition

$$u_1|_{in,\,ex}=u_{1_0}\sin(\omega t),\ u_2|_{in,\,ex}=u_3|_{in,\,ex}=0 \qquad (34)$$

(ii) Flather' s boundary condition (Flather, 1976)

$$u_1|_{in,\,ex}=u_{1_0}(t)\pm\frac{u_0}{u_0^2\,\rho_0}[p_D-p_{D_0}(t)],\ u_2|_{in,\,ex}=u_3|_{in,\,ex}=0 \qquad (35)$$

(iii) Orlanski' s boundary condition (Orlanski, 1976)

$$\frac{\partial u_1}{\partial t}\pm c\frac{\partial u_1}{\partial x}=0,\ u_2|_{in,\,ex}=u_3|_{in,\,ex}=0$$

$$c=\begin{cases} dx/dt\pm(du_1/dt)/(du_1/dx)>0 \\ 0\pm(du_1/dt)/(du_1/dx)\le 0 \end{cases} \qquad (36)$$

Orlanski' s boundary condition can be imposed for salinity and temperature on inflow/outflow boundaries.

Results and discussion

Internal waves derived by this numerical calculation are shown in Fig. 3. Internal wave starts to be generated centering the free surface near the edge part of the shelf in Fig. 3(a). And after that, the internal wave fluctuates with the period of half wave length as shown in Fig. 3(b). As time elapsed, it develops toward the deep sea with the formation of wave increasing periods as shown in Fig.3 (c) – (h).

Here, through the numerical calculation, it is seen that the maximum value of the vertical wave displacement is 40 – 70meters(wave amplitude: 20 – 35meters) during 2 – 32hours. It is in agreement with the estimations of Small et al.(1999). They found that

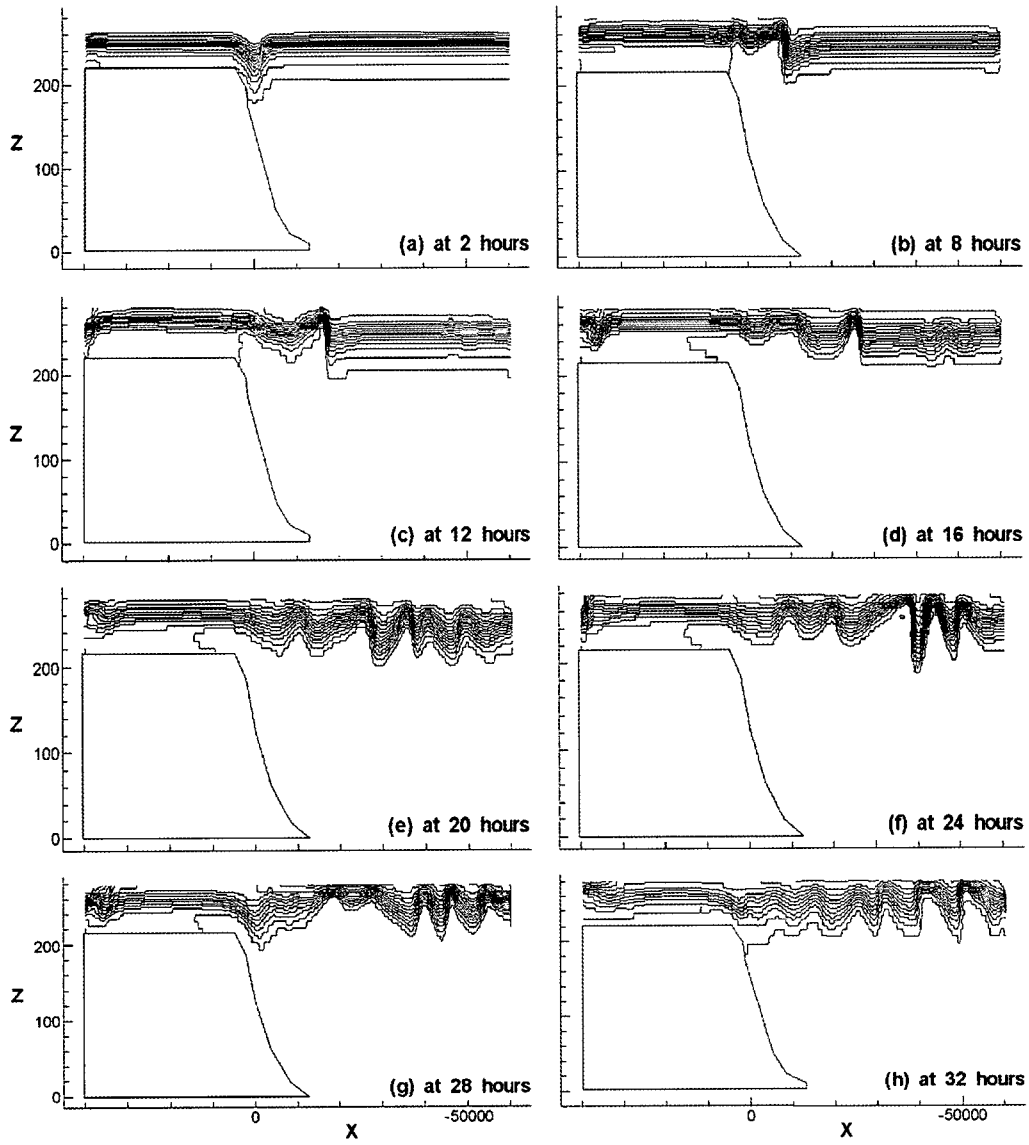

Fig. 3. Pattern of internal wave numerically calculated during 32 hours.

the wave amplitude must be at least 20meters, where their calculations were based on the analysis of SAR(Synthetic Aperture Radar) images and the results from a weakly nonlinear theory of internal waves. And for the phase speed of wave, using the mean amplitude of 27.5meters, it is calculated as about 0.9m/s.

And the result of numerical calculation on salinity distribution around the shelf is shown in Fig.4(a) – (b). As the flow patterns of salinity distribution at 12, 22 hours, show the same tendency as those of internal wave in Fig. 3(c) and (f), it can be seen that internal wave is generated in the close relationship with the density. And the result of numerical calculation on turbulent kinematic energy is shown in Fig.5(a) – (b).

It is shown that intensity of turbulence propagates

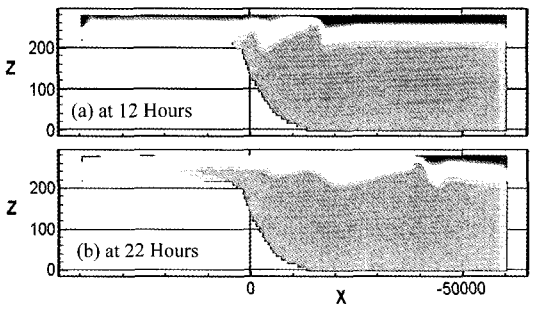

Fig. 4. Vertical section of the salinity field numerically calculated.

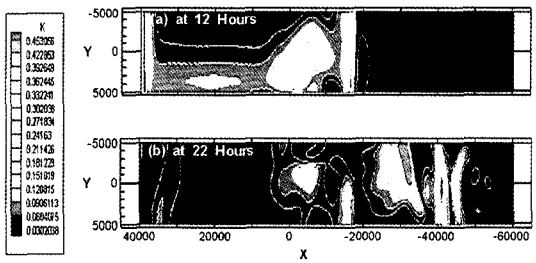

Fig. 5. Pattern of turbulent kinematic energy distribution.

centering the edge part of the shelf. Thus it is thought that the flow patterns of salinity distribution, temperature distribution, etc. are affected by such tendency of turbulent kinematic energy distribution.

Conclusion

The conclusions derived from the numerical calculation of this study are summarized as follows. The 3 – D modeling of ocean finite element method using k – ε turbulent model and tetrahedron grids has been set up to investigate the internal wave generation during the expansion of the deep water from the open sea to the shelf and then the numerical calculation of internal wave has been tried. From the results of the numerical calculation, internal wave was derived as the wave length of 15,000 – 20,000m, the wave height of 40 – 70m, the amplitude of 20 – 35m and the phase velocity of 0.9m/s. And the flow pattern of internal wave, salinity distribution and turbulence kinematic energy distribution were also derived. These values met the limit range suggested by Small et al.(1999) and showed the reliable tendency.

References

Belevich, M., 1996. The Effect of Thermal Stratification on the Structure of the Wave Boundary Layer. Izv. Atmos. Ocean. Phys., .32, 397 – 401.

Belevich, M., A. Safray, K.J. Lee and K.H. Kim, 2002. Wave boundary layer : Parameterization technique and its proof. Int. J. Ocean. Eng. and Tech., 16(2), 1020.

Flather, R.A., 1976. A tidal model of the Northwest European continental – shelf. Mem. Soc. R. Sci. Liege, Ser. 1 – 6, 10, 141 – 164.

Fletcher, C.A.J, 1991. Computational techniques for fluid dynamics. Springer – Verlag, 2, 552.

Kim, D.Y. and J.W. Kim, On the characteristics of internal waves between two stratified fluid layers. The Society of Naval Architects of Korea, 34(3), 1 – 8.

Mahadevan, A., Oliger J. and Street R., 1996, A nonhydrostatic mesoscale ocean model. Jour. of Phys. Oceangr. 26 1868 – 1880.

Muller, P., G. Holloway, F. Henyey and N. Pomphrey, 1986. Non – linear interactions among internal gravity waves. Reviews of Geophysics, 24, 493 – 536.

Norrie, D.H., D. Vries, 1978. An introduction to finite element analysis. Academic Press, 112.

Orlanski, I., 1976, A simple boundary condition for unbounded hyperbolic flows. J. Comput. Phys., 21, 251 – 269.

Safray, A.S. and I.V. Tkatchenko, 2001. Modeling the expansion of deep – sea water along area of arctic marginal sea. Research Activities in Atmospheric and Ocean Modeling, Rep. 31, 8.17, WMO/TD? No. 1064.

Schachverdi G.G., 1993. The impact interaction of ship construction with fluid. Sudostoenie, St. Petersburg, 256.

Small, J., Z. Hallock, G. Pavey and J. Scott, 1999. Observation of large amplitude internal waves at the marlin Shelf edge. Continental Shelf Research, 19, 1389 – 1436.

2005년 11월 1일 접수
2006년 1월 10일 수리